Monte Carlo Simulations of the Orientational Order in a Strained Polymer Network: Effect of Density

P. Sotta,* P. G. Higgs,† M. Depner, and B. Deloche

Laboratoire de Physique des Solides (CNRS-LA0002), Université Paris-Sud, 91405 Orsay, France, and Department of Physics, The University of Sheffield, Hicks Building, Hounsfield Road, Sheffield S37RH, United Kingdom

Received March 14, 1995; Revised Manuscript Received July 18, 1995⊗

ABSTRACT: Monte Carlo simulations are performed to investigate the uniaxial ordering of chain segments induced upon stretching a polymer network. The polymer network is modeled by chains with fixed extremities on a cubic lattice. Segmental interactions are introduced by imposing excluded volume between all segments in the system. A uniaxial contribution to orientation is shown to arise upon stretching even at a relatively low fraction of occupied sites Φ. This uniaxial contribution is studied as a function of Φ. The variation versus Φ is in agreement with that observed experimentally in a previous NMR work and is well described by a mean field model including orientation-dependent interactions between segments. It is shown additionally that a purely entropic model, including the packing entropy of segments, gives a mean field behavior qualitatively similar to that observed herein.

1. Introduction

Deuterium nuclear magnetic resonance (^{2}H NMR) has been used extensively to study the orientational order induced in rubber networks under uniaxial stress.[1−8] The spectrum of network chains exhibits a characteristic doublet structure. It was shown that the classical description of a network cannot explain the existence of such a doublet structure, which means that a uniaxial orientational field is generated in the system under the influence of the uniaxial stress. This effect has been attributed to orientational interactions between segments. These interactions give an energetic contribution to the overall segmental orientation, which is of the same order of magnitude as the classical entropic contribution but which results in modifying the local symmetry of the system, as perceived in segmental reorientational motions: most segments in the system are oriented on average along the applied constraint. A mean field model including such intersegmental interactions was proposed to describe this effect.[8]

Monte Carlo simulations of a model polymer system were performed to explain the occurrence of this orientational field and to clarify the nature of orientational interactions involved in this phenomenon.[9] The model system consisted of polymer chains on a cubic lattice. Fixed chain extremities are supposed to represent network junctions. Only isotropic excluded volume interactions between segments were introduced. It was demonstrated that the results of the simulations agree quite well with the mean field description mentioned above. In particular, it was found that a uniaxial contribution to segmental orientation is indeed generated in network chains upon stretching. This contribution is unambiguously related to excluded volume, since it vanishes when isolated chains are considered, i.e., when no interchain excluded volume is introduced in the system.[9]

The contribution of these segmental interactions to the segmental orientation depends on the polymer network volume fraction in the system. This was studied experimentally by measuring the orientational order generated in stretched networks diluted either with good solvent molecules or with free, homopolymer chains (i.e., chemically identical to network chains).[4] It was found that the uniaxial contribution to the order decreases when the polymer is more diluted, this decrease being much more pronounced when solvent molecules are used than when homopolymers are used.

In this paper, the influence of the polymer volume fraction Φ on the induced orientational order is investigated by Monte Carlo simulations. The same model system and Monte Carlo procedure as developed in ref 9 are used herein. Chains with fixed ends are simulated on a cubic lattice. The system is uniaxially elongated. Double occupancy of sites is disallowed. It is shown that the results of the simulations are in accordance with both experimental results obtained previously and the mean field model mentioned above.

However, the theoretical model given in ref 9 makes use of a finite interaction parameter between segments, which may appear somewhat artificial, since no finite energy is introduced in the simulated system. The effect observed in the simulations might be purely entropic, having its origin in the restrictions which occur when packing a large number of segments in a box. The variation of this translational entropy of segments is estimated. It is shown that, within a mean field treatment, this additional entropic contribution gives indeed a uniaxial part in the orientation, with a variation versus Φ comparable to the observed one. The agreement, however, is not quantitative.

The paper is organized as follows. The mean field theory and the Monte Carlo method are described in section 2. Specifically, the quantities which are measured, in connection to NMR experiments, are detailed. The results are presented and compared to the mean field model in section 3. In section 4, the contribution to orientation, originating in the packing entropy of chain segments, is estimated and compared to the results of the simulations.

2. Model and Computer Simulations

2.1. Distribution Function of Orientation. The ^{2}H NMR frequency spectrum $S(\omega)$ observed in a locally

* To whom correspondence should be sent. Present address: Max-Planck-Institut für Polymerforschung, Postfach 3148, D-55021 Mainz, Germany.

† Department of Physics, The University of Sheffield.

⊗ Abstract published in *Advance ACS Abstracts,* September 1, 1995.

0024-9297/95/2228-7208$09.00/0

anisotropic system is given by[9]

$$S(\omega) \sim \varrho(\Delta) + \varrho(-\Delta) \quad (1)$$

where $\varrho(\Delta)$ is the distribution function for the segmental orientation. Δ is given by

$$\Delta = \omega/\nu_Q = \left\langle \frac{3\cos^2\Theta - 1}{2} \right\rangle \quad (2)$$

Θ is the angle between a given segment and the direction of the static magnetic field $\mathbf{B}_0$. In all this paper, the orientation will be calculated with respect to the anisotropy direction 3, which would correspond to applying the external force parallel to $\mathbf{B}_0$ in the actual experiment. In the ^{2}H NMR experiment, brackets denote a temporal average over molecular motions faster than the inverse of the static quadrupolar interaction ν_Q, i.e., faster than 10^{-5} s. The validity of eqs 1 and 2 relies on the assumption that intrachain segmental motions are within this fast motion limit, whereas end-to-end vectors are fixed on average.[10,11] This seems to be clearly the case in the PDMS networks which have been studied experimentally.[12] Then the temporal average in eq 2 may be equivalently computed as a statistical intrachain average, the extremities of the chains being fixed.

2.2. Mean Field Model. It was already pointed out that the spectrum corresponding to eq 1 presents very different features in the absence or presence of excluded volume interactions.[9] Whereas no doublet appears in the absence of interchain excluded volume (isolated chains), a well-resolved doublet with half-splitting Δ_{uniax} appears when excluded volume is switched on, thus allowing a direct measurement of the quantity Δ_{uniax}. In other words, the distribution $\varrho(\Delta)$ has its maximum at a nonzero value Δ_{uniax}. This doublet corresponds to the one which has been observed experimentally in rubber networks. It was interpreted by a mean field model including both entropic chain elasticity and a uniaxial orientational field of quadrupolar symmetry induced upon stretching. In this model, this uniaxial field results from presumably short-range, orientation-dependent interactions between chain segments. It is included in the network free energy via a Maier–Saupe term. The average segmental orientation calculated with respect to the anisotropy direction for one chain p on a cubic lattice, with a fixed end-to-end vector $\mathbf{R}$ of components x_1, x_2, and x_3, in a uniaxially stretched network, is expressed as[9]

$$\Delta_p = \kappa\left(\frac{3}{4N^2}(2x_3^2 - x_1^2 - x_2^2) + \frac{\beta}{3}\right) \quad (3)$$

The first term in the sum is the classical entropic contribution. It is related to the anisotropy induced along the chain by the constraints on extremities. The second term represents the effect of the mean field. The uniaxial contribution

$$\Delta_{uniax} = \kappa\frac{\beta}{3} \quad (4)$$

corresponds to half of the doublet splitting. The factor κ is introduced to account for intrachain first-neighbor interactions, related to the fact that perpendicular relative orientation for two successive segments along a chain is artificially favored on a cubic lattice. The value for κ which was found from the simulations in ref 9 is $0.65 < \kappa < 0.7$. It should be noticed that this value is in excellent agreement with that predicted in ref 13 for chains on a cubic lattice with nearest-neighbor interactions, i.e., $\kappa = 2/3$, based on an analogy between the description of chains with nearest-neighbor interactions and that of binary copolymerization.[14] This value will be used in the following.

Equation 3 has to be complemented with a self-consistency condition, which expresses that β itself should be proportional to the orientation averaged over the whole system:

$$\beta = 3v\langle\Delta\rangle \quad (5)$$

$\langle\Delta\rangle$ is the orientation as given in eq 3, averaged over the whole system. v is a local interaction parameter, which may depend on the volume fraction of polymer network Φ. It is this dependence which is investigated herein.

The uniaxial contribution Δ_{uniax} may be expressed alternatively in terms of the average orientation $\langle\Delta\rangle_{Gaussian} = (\lambda^2 - \lambda^{-1})/2N$ which is expected in a Gaussian, unswollen, phantom network, without interactions:

$$\Delta_{uniax} = \frac{\kappa^2 v}{1 - \kappa v}\langle\Delta\rangle_{Gaussian} \quad (6)$$

Two quantities are relevant in order to characterize the induced orientation in the system. One is the uniaxial contribution Δ_{uniax}. The other one is the mean orientational order $\langle\Delta\rangle$ averaged over the whole network. Note that measuring only that latter quantity would not provide the essential information on the induced uniaxiality in the system.

2.3. Variation versus the Polymer Volume Fraction. In a network diluted with a solvent (network volume fraction Φ), the term in the free energy which describes local interactions involves three different parameters, u_{pp} for segment–segment, u_{ss} for solvent–solvent, and u_{ps} for polymer–solvent interactions. This enthalpic term may be written, per site[4]

$$F_{int} = -\frac{\Phi^2}{2}u_{pp}S_p^2 - \frac{(1-\Phi)^2}{2}u_{ss}S_s^2 - \Phi(1-\Phi)u_{ps}S_pS_s \quad (7)$$

The index p denotes network chain segments and s solvent molecules, which may be eventually free homopolymer chain segments. The quantities S_j's are orientational order parameters. For each species j, S_j should be identified with the average orientation $\langle\Delta\rangle_j$, in similarity with eq 5. However, the introduction of interaction parameters u_{ss} and u_{ps} appears quite irrelevant in the framework of the present simulations, since solvent molecules are more or less (though not exactly, since a system with $\Phi = 1$ would be frozen) assimilated to empty lattice sites, whose orientation is impossible to define. Therefore the u_{pp} parameter only is kept nonzero (the notation $u_{pp} = 3v_0$ is adopted in the following). Given this simplification, the explicit Φ dependence of the uniaxial part of the orientational order is given by

$$\Delta_{uniax} = \kappa\Phi v_0\langle\Delta\rangle \quad (8)$$

or:

$$\Delta_{\text{uniax}} = \frac{\kappa^2 \Phi v_0}{1 - \kappa \Phi v_0} \langle \Delta \rangle_{\text{Gaussian}} \tag{9}$$

These formulas are the same as in ref 9 with v replaced by Φv_0, as could be expected from the structure of the interaction term, eq 7. Thus, in this model, the ratio $\Delta_{\text{uniax}}/\langle \Delta \rangle$ as a function of Φ gives a straight line of slope κv_0.

2.4. Monte Carlo Method. The model system used herein is the same as in ref 9. N_c sites (fixed initial beads of the N_c chains) are randomly distributed in a box on a cubic lattice. The uniaxially deformed system is contained in a box uniaxially elongated along direction 3; that is, the dimensions of the box are $L_1 = L_2 = \lambda^{-1/2} L_0$, $L_3 = \lambda L_0$, where λ is the deformation ratio. The terminal beads of the chains are then generated. End-to-end vector components x_1, x_2, x_3 are supposed to be affinely deformed; i.e., the components obey the following distributions:

$$p(x_i) \approx \exp\left[-\frac{x_i^2}{2\sigma_i^2}\right] \tag{10}$$

with $\sigma_1^2 = \sigma_2^2 = \lambda^{-1}\sigma_0^2$, $\sigma_3^2 = \lambda^2 \sigma_0^2$, and $\sigma_0^2 = \langle x_i^2 \rangle_0 = N/3$.

Chains of a given length N sites (or $N - 1$ segments) are then generated. The polymer volume fraction Φ (fraction of occupied sites) is related to the number of chains in the box by $\Phi = N_c N/V$, where $V = L_1 L_2 L_3$ is the total number of sites in the box.

Two types of unit moves are used to generate different conformations in the Monte Carlo algorithm: L inversions and modified kink shifts, which allow long-range transport of kinks along one chain.[15-17] One unit MC move obeys the following procedure: one chain is chosen at random. One type of move is then selected at random, with probability $1/2$. In the selected chain, one of the segments which allows the selected type of move to be attempted is then chosen at random. The move is successful if the excluded volume condition (no multiple occupancy of each site) is fulfilled. Chain extremities are kept fixed. Periodic boundary conditions are applied.[18] The parameters used are typically the following: box dimensions $10 \times 10 \times 70$, which corresponds to an elongation ratio $\lambda = 3.66$; chain length $N = 49$ sites; number of chains in the box $N_c = 1-120$ ($\Phi = 0.84$).

A preliminary run is performed to reach a good starting random configuration. The number of steps in this initial run is estimated in the following way. The largest relaxation time for a chain of length N is of the order $\tau = 0.25N^{3.13}$ elementary MC steps.[19,20] This represents the time needed to explore the configurational space for a free chain. Note that the relaxation time may be expected to be significantly shorter for chains with fixed ends, whose configurational space is smaller. Thus, for chains with $N = 49$ sites, $\tau \sim 5 \times 10^4$, and for a system of N_c chains ($N_c \sim 100$), the relaxation time will be of the order $N_c\tau \sim 5 \times 10^6$. The equilibration time in the initial run was therefore chosen to be of the order $5-10\ N_c\tau$ (i.e., typically 25×10^6 for 100 chains of length 49). It was checked that a stationary value has been reached for the measured quantities.

The number of attempted steps in the MC runs themselves is typically 10^9, which corresponds to a few 10^5 attempted moves per segment. To construct the distribution function $\varrho(\Delta)$, the average orientation Δ, as given in eq 2, is measured for each segment in the system. It is averaged over typically a few 10^4 configurations, which means that values are extracted every 50 attempted moves per segment. Finally, in each case, the results are averaged over several different systems in order to have an overall number of chains between 240 and 400.

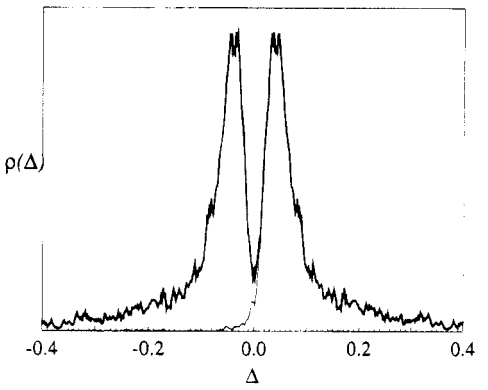

Figure 1. Spectrum obtained as the symmetrized distribution function $\varrho(\Delta) + \varrho(-\Delta)$. The distribution $\varrho(\Delta)$ is also represented. Elongation rate $\lambda = 3.66$, chain length $N = 48$ segments, volume fraction $\Phi = 0.84$.

3. Results

3.1. Uniaxial Contribution to Orientation. One example of a spectrum is plotted in Figure 1 for $N = 48$ segments, $\lambda = 3.66$, and $\Phi = 0.84$. It appears immediately that it is rather difficult to measure the doublet splitting with a good accuracy. Though the spectrum is well resolved, the line width is quite comparable to the splitting itself. Note that the apparent noise in the spectrum is related to the discrete character of the end-to-end vector distribution. Thus, to obtain a better insight into the distribution function of orientation in the system, the following method is used. The quantity Δ, measured for each segment, is first averaged along each chain. Segments close to extremities are excluded to avoid any end effects.[9] Typically four segments at each extremity are excluded. Then the quantity Δ, averaged for each chain, is plotted as a function of the quantity $\eta = (3/4N^2)(2x_3^2 - x_1^2 - x_2^2)$. According to eq 3, a straight line of slope κ should be obtained and the uniaxial contribution Δ_{uniax} should be given by the intercept at $\eta = 0$. In the case $\Phi = 0$, where the uniaxial contribution vanishes ($\beta = 0$), the line should cross the origin. The case $\Phi = 0$ is modeled by a simulation wherein only nearest-neighbor interactions are present: overlapping of two successive segments along one chain is forbidden, whereas no excluded volume is imposed between segments which are not directly connected. In that case, eq 3 is well verified by the simulation. This was checked in ref 9, and the value $\kappa = 0.70$ was obtained in that case.

However, the mean field effect leading to the β term in eq 3 essentially originates in the interactions between segments belonging to different chains. Therefore, we choose herein to distinguish interchain and intrachain excluded volume interactions. In Figure 2, the curve Δ versus η is plotted for isolated chains: excluded volume is imposed between all segments of each chain, whereas there is no excluded volume between segments belonging to distinct chains. This curve deserves some comments. It is clear that at high η values (typically $\eta > 0.1$) the linear regime in eq 3 is no longer fulfilled and

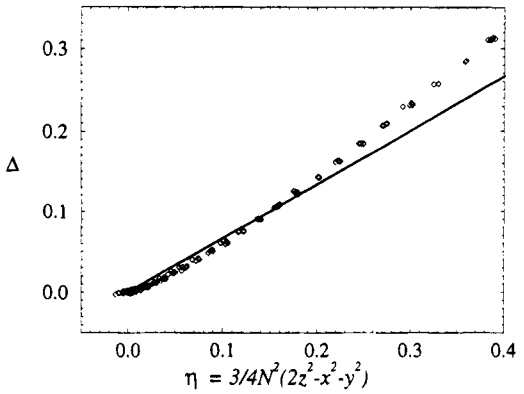

Figure 2. Orientation Δ averaged for each chain plotted versus $\eta = (3/4N^2)(2x_3^2 - x_1^2 - x_2^2)$ for $\lambda = 3.66$ and $N = 48$ segments in the case of isolated chains with excluded volume. The straight line corresponds to eq 3 with $\kappa = 2/3$ and $\beta = 0$.

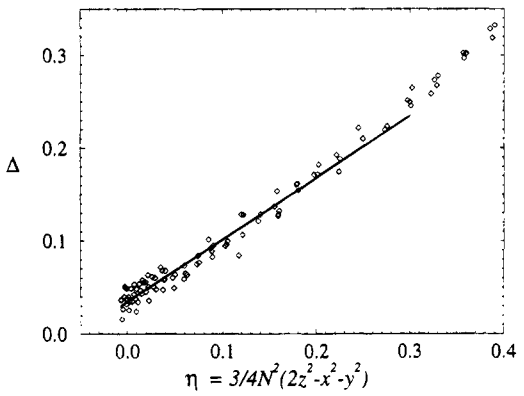

Figure 3. Orientation Δ averaged for each chain plotted versus $\eta = (3/4N^2)(2x_3^2 - x_1^2 - x_2^2)$ for $\lambda = 3.66$, $N = 48$ segments, and $\Phi = 0.84$. The straight line is the best fit with eq 3 and $\kappa = 2/3$, obtained for chains with $\eta < 0.3$.

higher order terms in η should be included. However, at low η values also, the curve is clearly different from the straight line drawn according to eq 3. The effect of intrachain excluded volume is to decrease the measured orientation with respect to what is expected for ideal chains, especially for chains with small end to end distances.

In Figure 3 the curve Δ versus η is plotted in the case of a rather high density, $\Phi = 0.84$. Excluding volume between all segments is applied. The curve which is obtained is roughly parallel to the curve in Figure 2. This point emphasizes nicely the mean field assumption underlying eq 3. Note that no large negative η values appear in Figure 2 or 3, due to the high elongation ratio.

Thus, only chains with small η values (typically smaller than 0.1) should be considered. The curves Δ versus η are fitted with a straight line of slope $\kappa = 2/3$ and the ordinate at $\eta = 0$ is taken as the uniaxial contribution Δ_{uniax}. The dispersion of points in the curves Δ versus η being quite large in the case $\Phi \neq 0$, large uncertainties remain in this procedure. It should be noted that this dispersion does not come from an incomplete averaging of segmental orientation but rather from packing restraints which prevent the entropic part in the orientation (first term in the sum in eq 3) to being strictly averaged along the end-to-end vector. In other words, the chain cannot explore all the configurations which would be accessible if it was isolated.

3.2. Variation versus Volume Fraction. We focus herein on the dependence of the uniaxial contribution Δ_{uniax} on Φ, the volume fraction of polymer network

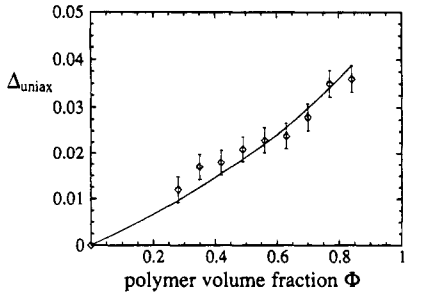

Figure 4. Dependence of the uniaxial part Δ_{uniax} of the average orientation of chain segments on the volume fraction Φ. The curve corresponds to eq 9 with $v_0 = 0.6$.

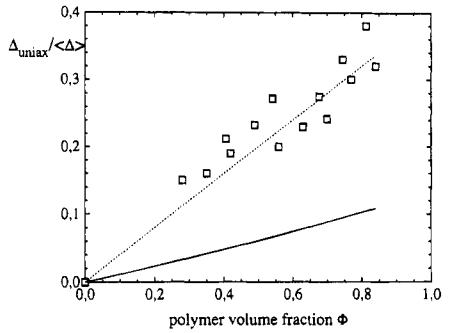

Figure 5. Ratio $\Delta_{uniax}/\langle\Delta\rangle$, where $\langle\Delta\rangle$ is the mean orientation averaged over the system, plotted versus the volume fraction Φ. Two series of simulations are shown: $\lambda = 3.66$, $N = 48$ segments and $\lambda = 2.23$, $N = 38$ segments, the latter being normalized to the same λ and N using the Gaussian, phantom value. The dashed line corresponds to eq 8 with $v_0 = 0.6$ and $\kappa = 2/3$, and the continuous one to eq 18.

chains. The spectra were computed by the MC method for systems with different volume fraction Φ, the box dimensions and elongation parameter λ being kept constant. The end-to-end vector distribution, given in eq 10, is also kept constant in all systems, i.e., independent of Φ. Therefore, no swelling effect is introduced and the quantity which is measured is related only to the variation in local ordering properties.

In Figure 4, the uniaxial contribution Δ_{uniax}, measured as explained above, is plotted as a function of Φ. The curve $\Delta_{uniax}(\Phi)$ increases from $\Delta_{uniax} = 0$ at $\Phi = 0$ to a maximum value at the maximum value investigated, $\Phi = 0.84$. The value at $\eta = 0$ in the curve $\Delta(\eta)$, or equivalently the maximum in the distribution $\varrho(\omega)$ (eq 3 or 1), remains clearly different from zero even at rather low Φ values. Thus, it is remarkable that the mean field effect persists over a relatively large range of volume fraction.

The ratio $\Delta_{uniax}/\langle\Delta\rangle$, the average $\langle\Delta\rangle$ being taken over all chains in the system, is plotted as a function of Φ in Figure 5. According to eq 8, this procedure minimizes the influence of the end-to-end vector distribution. It should be noted that the average orientation $\langle\Delta\rangle$ obtained in the present simulations, in the case of isolated chains, is systematically larger than the Gaussian value $\langle\Delta\rangle_{Gaussian}$. This probably comes from the fact that a significant part of the chains are not in the linear regime of eq 3, and higher order terms should be included to compute $\langle\Delta\rangle$.

4. Discussion

4.1. Orientational Interactions versus Isotropic Interactions. The results obtained by the MC method in the present simulations correspond to what was observed experimentally in PDMS networks diluted

with solvent molecules.[4] A decrease in the uniaxial orientational order as perceived in ^2H NMR spectra was observed when the networks were diluted, and the curve $\Delta_{uniax}(\Phi)$ obtained herein is qualitatively similar to that obtained experimentally in ref 4.

The results obtained in the present simulations are now compared to the prediction of the mean field model recalled in section 2. The value $\kappa = {}^2/_3$ is adopted, in accordance with refs 9 and 13. Though the scattering of data points in Figure 5 is rather important, it is relevant to compare the variation versus Φ to eq 8, which predicts a linear variation. The slope obtained from fitting the results in Figure 5 with eq 8 gives the value $v_0 \cong 0.6$. This value is in agreement with that found in ref 9, which must be read, given the notation adopted in the present work, $v = \Phi v_0 \cong 0.5$, with $\Phi \cong 0.8$ in ref 9.

However, in the mean field description presented above, the interaction term F_{int} is written in terms of orientational parameters S_j's, even though the excluded volume interaction in the simulation is isotropic. It would possibly be more appropriate to express F_{int} in terms of density variables. Such a model was considered in detail by Brereton in refs 21 and 22. It was shown to also give rise to an NMR doublet in a uniaxially deformed system, due to anisotropic screening of the excluded volume potential. The splitting was calculated as a function of the Edwards screening length ξ.[23] The spatial scales at which local interactions are considered are quite different in both approaches, since the Brereton theory considers the chains at the spatial scale of Gaussian subchains, i.e., at a larger scale than in the present work. In the case of a blended network, the splitting is predicted to increase as the network volume fraction increases. Thus the present result seems to be in agreement with this prediction.

4.2. Role of Packing Entropy. It is difficult to relate directly the coupling constant v_0 (or the excluded volume parameter in the Brereton theory) to any quantity in the simulation. Indeed, since no finite interaction energy between segments was introduced in the simulation, the uniaxial order which we observe must arise from a purely entropic effect. The situation is similar to simulations of hard rigid rods, where it is known that if the density is sufficiently high, the rods will spontaneously order into an aligned nematic state. This is because the translational entropy is maximized in the aligned state. In the networks studied here, there is no spontaneous alignment since the molecules do not contain rigid mesogenic units. However, straining the network causes a partial alignment of the segments, and we suggest that the segments will maximize their entropy by increasing their degree of orientation along the strain direction. In other words, the uniaxial order which is observed arises due to the constraints of packing together many segments which are already partially aligned due to deformation of the network.

In this section we give an argument to show that the coupling constant in the mean field theory may arise purely from entropic effects. We follow the framework of calculations by Di Marzio.[24-26] The idea is to take into account the decrease in both the orientational entropy due to junctions, which is the usual elastic contribution, and the translational entropy. The translational entropy as a function of the orientational distribution of the segments has been computed in refs 24-26. The average orientation resulting from this effect in a stretched network was calculated by Tanaka and Allen.[13] However, the uniaxial character of the segmental orientation was not considered in that work. Both entropy terms were treated separately. Thus, we propose to analyze this entropic effect, taking into account the uniaxiality in the system. The total entropy, as the sum of these two terms, will be estimated within a mean field assumption and maximized.

The starting point is the estimation of the conditional probability that a site A is empty, given that an adjacent site B is empty. If the system is anisotropic, this probability p_i depends on the direction i of the segment connecting A to B. If N_c chains of length N sites are placed on a lattice containing $V = N_0 + N_cN$ sites in total, with an overall fraction α_i of the segments lying in direction i, p_i is given by[24]

$$p_i = \frac{N_0}{V - (N-1)N_c\alpha_i} \tag{11}$$

Note that p_i is larger than the probability that site A is empty, which is simply N_0/V (N_0 is the number of empty sites). This is so because if B is not empty, the polymer chain which occupies B may jump into A. This probability p_i is given herein as an average probability in the system, in a mean field assumption. Now one may compute the entropy reduction of one given chain, due to the presence of all other chains. The average number of ways to place this chain, all other chains being already placed on the lattice, is given by

$$C = N_0 \prod_i \left[\frac{N_0}{V - (N-1)N_c\alpha_i}\right]^{(N-1)f_i} \tag{12}$$

The orientational distribution function for the given chain is denoted by f_i, while the overall distribution function in the system is α_i. The product with index i takes into account all six possible orientations and directions for one segment. Segments pointing in the $+i$ direction (superscript +) have to be distinguished from those pointing in the $-i$ direction (superscript −). For symmetry reasons, $\alpha_i^+ = \alpha_i^- = \alpha_i$, whereas this is not the case for f_i: a priori $f_i^+ \neq f_i^-$. The consistency of the mean field assumption is ensured by assuming that

$$\alpha_i = \left\langle \frac{1}{2}(f_i^+ + f_i^-) \right\rangle = \frac{1}{2N_c}\sum_p (f_i^+ + f_i^-) \tag{13}$$

where the summation extends over all chains in the system. The "entropy of packing" for the chain is then estimated as

$$\frac{S_{pack}}{k_B} = \ln C = \ln \frac{N_o^N}{\prod_i [V - (N-1)N_c\alpha_i]^{(N-1)f_i}} \tag{14}$$

which gives in the limit $N \gg 1$

$$\frac{S_{pack}}{k_B} = N \ln N_0 - N \ln V - N\sum_i f_i \ln[1 - \Phi\alpha_i] \tag{15}$$

$\Phi = (N_cN)/V$ is the fraction of occupied sites (volume fraction) in the lattice.

The orientation-dependent free energy for a given chain with fixed ends is thus per segment (expressed in k_BT units)

$$G = \sum_{i=1}^{3} f_i^+ \ln f_i^+ + f_i^- \ln f_i^- - \mu_i(f_i^+ - f_i^-) + f_i^+ \ln(1 - \Phi\alpha_i) + f_i^- \ln(1 - \Phi\alpha_i) \quad (16)$$

The first two terms represent the usual orientational entropy. The μ_i term is the Lagrange term accounting for the condition that extremities are fixed.[8,9] The last two terms come from the packing entropy, eq 15. The segmental orientation obtained after minimization of G is (see Appendix)

$$\Delta = \left(\frac{3}{4N^2}(2x_3^2 - x_1^2 - x_2^2) + \frac{\beta}{3}\right) \quad (17)$$

with

$$\frac{\beta}{3} = \frac{\Phi\langle\Delta\rangle}{6 - \Phi} \quad (18)$$

If nearest-neighbor interactions within one chain are taken into account, the orientation may be written in the same way as before:

$$\Delta = \kappa\left(\frac{3}{4N^2}(2x_3^2 - x_1^2 - x_2^2) + \frac{\beta}{3}\right) \quad (19)$$

with β still given by eq 18. The structure of this result is the same as in eq 3. However, no adjustable parameter (interaction coupling constant) appears in the uniaxial contribution. In this model, the resulting orientation results from a competition between two entropic contributions. While the first term (orientational entropy) tends to favor an orientational configuration as disordered as possible, the second one (translational entropy) tends to increase the orientational order so as to increase the number of translational configurations accessible to segments. Though not strictly linear, the variation versus Φ given in eq 18 is not strongly different from that in eq 8, in the interval of physically relevant values $0 < \Phi < 1$. Specifically the induced order Δ_{uniax} is zero for all values of the volume fraction when the network is unstrained. No spontaneous ordering (nematic-like transition) is therefore expected to occur in this model, in agreement with the theory by Brereton,[21] also based on isotropic interactions.

The result given in eq 18 may be directly compared to the results of the simulations. This is done in Figure 5. Though the variation $\Delta_{uniax}(\Phi)$ is reproduced quite accurately, the measured values of the uniaxial ordering are typically 3 times larger than predicted, which is well outside error bars. Thus, the above theory does not quantitatively explain the results, even though no explicit orientational interaction is present in the system under study. This discrepancy is probably due to the mean field assumptions underlying eq 14, which may be too crude, since there is no energy or anything else in the simulation.

5. Conclusion

Segmental orientation induced in strained polymer networks are studied by Monte Carlo simulations on a cubic lattice. The present work is a part of Monte Carlo studies initiated in ref 9. The uniaxial contribution to segmental orientation is analyzed as a function of the polymer volume fraction Φ. The results are found to be in good agreement with the mean field description including orientation-dependent interactions between segments, developed previously. Specifically, the decrease of orientation when the system is diluted is satisfactorily accounted for. Then, it is shown that an interpretation based on purely entropic considerations does predict a uniaxial contribution to the orientation, with the correct variation versus Φ. No energetic adjustable parameter is needed in this interpretation. However, the agreement with the results of the simulations is not quantitative.

Though in the present simulations only entropic effects are probably present, both entropic and enthalpic effects may give a contribution to the orientation measured by ^{2}H NMR in rubber networks. However, since both effects give relatively similar variation versus Φ, they may be difficult to distinguish experimentally. To distinguish enthalpic effects (as described by eq 5) from entropic effects (eq 18), it would possibly be interesting to vary experimentally the quality of the solvent, i.e., the interaction parameter v. In this case a pronounced variation of the uniaxial contribution to orientation would possibly indicate that enthalpic effects are predominant.

Acknowledgment. P.S. thanks the Sheffield Centre for Molecular Materials for financial support.

Appendix

The distribution function obtained by minimizing the free energy G (eq 16) is

$$f_i^{\pm} = \frac{1}{Z}\exp[\pm\mu_i - \ln(1 - \Phi\alpha_i)] \quad (A1)$$

The partition function Z is

$$Z = \sum_{i=1}^{3}\exp[+\mu_i - \ln(1 - \Phi\alpha_i)] + \exp[-\mu_i - \ln(1 - \Phi\alpha_i)] = \frac{2}{1 - \Phi\alpha_1}[\cosh\mu_1 + \cosh\mu_2 + \exp\beta\cosh\mu_3] \quad (A2)$$

with

$$\exp\beta = \frac{1 - \Phi\alpha_1}{1 - \Phi\alpha_3} \quad (A3)$$

From eq 13, the overall averaged orientation $\langle\Delta\rangle$ may be related to the α_i's by

$$\langle\cos^2\theta\rangle = \left\langle\frac{1}{2}(f_3^+ + f_3^-)\right\rangle = 2\alpha_3 \quad (A4)$$

so that

$$\alpha_1 = \alpha_2 = \frac{1 - \langle\Delta\rangle}{6}; \qquad \alpha_3 = \frac{1 + 2\langle\Delta\rangle}{6} \quad (A5)$$

Z may be expanded in a series of μ_i and β, under the assumption that $\langle\Delta\rangle$, and therefore β, is small. Then, in first order

$$\frac{x_i}{N} = \frac{1}{Z}\frac{\partial Z}{\partial\mu_i} = \frac{\mu_i}{3} \quad (A6)$$

so that Z, expanded in a series of x_i/N and β, may be replaced in eq A1, leading to

$$f_{1,2}^{\pm} = \frac{1}{6}\left[1 - \frac{3}{2N^2}(x_1^2 + x_2^2 + x_3^2) - \frac{\beta}{3}\right] \times \left[1 \pm \frac{3}{N}x_{1,2} + \frac{9}{2N^2}x_{1,2}^2\right] \quad \text{(A7a)}$$

$$f_3^{\pm} = \frac{1}{6}[1 + \beta]\left[1 - \frac{3}{2N^2}(x_1^2 + x_2^2 + x_3^2) - \frac{\beta}{3}\right] \times \left[1 \pm \frac{3}{N}x_3 + \frac{9}{2N^2}x_3^2\right] \quad \text{(A7b)}$$

The segmental orientation is then given by

$$\Delta = f_3^+ + f_3^- - \frac{1}{2}(f_1^+ + f_1^- + f_2^+ + f_2^-) \quad \text{(A8)}$$

which leads to eqs 17 and 18 in the text.

References and Notes

(1) Deloche, B.; Samulski, E. T. *Macromolecules* **1981**, *14*, 575.
(2) Deloche, B.; Beltzung, M.; Herz, J. *J. Phys. Lett.* **1982**, *43*, 1763.
(3) Sotta, P.; Deloche, B.; Herz, J.; Lapp, A.; Durand, D.; Rabadeux, J. C. *Macromolecules* **1987**, *20*, 2769.
(4) Sotta, P.; Deloche, B.; Herz, J. *Polymer* **1988**, *29*, 1171.
(5) Gronski, W.; Stadler, M.; Jacobi, M. *Macromolecules* **1984**, *17*, 741.
(6) Jacobi, M.; Stadler, R.; Gronski, W. *Macromolecules* **1986**, *19*, 2887.
(7) Litvinov, V.; Spiess, H. W. *Makromol. Chem.* **1992**, *193*, 1181.
(8) Sotta, P.; Deloche, B. *Macromolecules* **1990**, *23*, 1999.
(9) Depner, M.; Deloche, B.; Sotta, P. *Macromolecules* **1994**, *27*, 5192.
(10) Cohen-Addad, J. P.; Dupeyre, R. *Polymer* **1983**, *24*, 400.
(11) Samulski, E. T. *Polymer* **1985**, *26*, 177 and references cited therein.
(12) Sotta, P.; Deloche, B. *J. Chem. Phys.* **1994**, *100*, 4591.
(13) Tanaka, T.; Allen, G. *Macromolecules* **1977**, *10*, 426.
(14) Stockmayer, W. H. *J. Chem. Phys.* **1945**, *13*, 199.
(15) Kremer, K.; Binder, K. *Comput. Phys. Rep.* **1988**, *7*, 259.
(16) Reiter, J.; Edling, T.; Pakula, T. *J. Chem. Phys.* **1990**, *93*, 837.
(17) Reiter, J. *Macromolecules* **1990**, *23*, 3811.
(18) Binder, K. *Monte Carlo Methods in Statistical Physics*; Springer-Verlag: Berlin, 1979.
(19) Chakrabarti, A.; Toral, R. *Macromolecules* **1990**, *23*, 2016.
(20) Gurler, M. T.; Crabb, C. C.; Dahlin, D. M.; Kovac, J. *Macromolecules* **1983**, *16*, 398.
(21) Brereton, M. G. *Macromolecules* **1993**, *26*, 1152.
(22) Brereton, M. G. *Makromol. Chem., Macromol. Symp.* **1993**, *76*, 249.
(23) Edwards, S. F. *J. Phys. A* **1975**, *8*, 1670.
(24) Di Marzio, E. A. *J. Chem. Phys.* **1961**, *35*, 658.
(25) Di Marzio, E. A. *J. Chem. Phys.* **1962**, *36*, 1563.
(26) Di Marzio, E. A. *Macromolecules* **1991**, *24*, 1595.

MA950330H